Available online at www.sciencedirect.com

SciVerse ScienceDirect

Ceramics International 38 (2012) 3227–3235

CERAMICS INTERNATIONAL

www.elsevier.com/locate/ceramint

Fabrication and characterization of anorthite-based ceramic using mineral raw materials

Xiaosu Cheng, Shanjun Ke *, Qianghong Wang, Hui Wang, Anze Shui, Pingan Liu

College of Materials Science and Engineering, South China University of Technology, 510640, Guangzhou, Guangdong, China

Received 7 December 2011; received in revised form 12 December 2011; accepted 13 December 2011
Available online 19 December 2011

Abstract

The purpose of this study is to design a novel single crystalline phase ceramic based on anorthite whose properties fulfill the tableware market requirements such as high appearance quality, strength and thermal shock resistance. To obtain the single phase anorthite ceramic, ball clay, quartz, calcite, feldspar and alumina were used as raw materials. The single phase anorthite ceramic was fabricated by slip casting and sintering at 1230 °C for 1 h. It has a high flexural strength of 103 MPa, which is higher than that of the conventional porcelain. The single phase anorthite ceramic had relatively low (4.9×10^{-6} K^{-1}) thermal expansion coefficient which can be matched with applicable glaze easily. Furthermore, the single phase anorthite ceramic had high degree of whiteness ($L^* = 94$) and excellent translucency behavior which could achieve a high-quality decorative effect.

Keywords: Anorthite-based ceramics; Ceramic tableware; Porcelain

1. Introduction

Anorthite ($CaAl_2Si_2O_8$) is one of the most important members of the plagioclase feldspar family [1], which is a crucial component of substrate materials in electronics industry as it possesses good physical properties such as low thermal expansion coefficient, high thermal shock resistance and low dielectric constant [2–4]. With these excellent characteristics, the application fields of anorthite ceramics have been observed to expand to electronics industry, industrial heat exchangers and biomedical materials [5,6]. But the natural anorthite is a rare material that cannot be mined in mass tonnages and also the quality of the material does not satisfy the industrial demand. So, anorthite should be synthetically produced from inexpensive raw materials.

Usually, synthesis of anorthite was extensively studied by using different methods such as sintering of mixtures, mechanochemical treatments and sol–gel. All these methods carry their own advantages and disadvantages [7–9]. According to CaO–Al_2O_3–SiO_2 phase diagram, pure anorthite has a melting point of 1553 °C [10], which makes the synthesis of pure anorthite at a relatively low temperature difficult. Several studies [8,9,11–13] were carried out in order to decrease the firing and crystallization temperature by employing different fluxing agents like B_2O_3, Na_2CO_3, MgO, $MgCO_3{\cdot}Mg(OH)_2{\cdot}5H_2O$ and $2CaO_3{\cdot}B_2O_3{\cdot}5H_2O$. In addition, controlling the particle size of the raw materials also led to the production of dense anorthite ceramics with a relatively low temperature [8,14]. Meanwhile, anorthite has a refractive index of 1.58 [15], which is close to that of glass phase at ~1.51 [16]. The low relative refractive index between crystalline and glassy phase can make anorthite ceramic own excellent property of translucency, which has an appearance comparable with bone china. Therefore, anorthite ceramic was applied in tableware porcelain in order to improve its service performance and decoration quality.

Especially, Capoglu [17–19] designed a low-clay translucent whiteware, which was produced from coarsely and finely milled prefired materials of the same composition plus a small amount of clay at 1370 °C for 3 h. The low-clay whiteware consisted of anorthite and mullite ($3Al_2O_3{\cdot}2SiO_2$) crystalline phases and a glassy phase with high crystalline to glassy phase ratio. And the flexural strength could reach ~110 MPa. Capoglu and Ustundag [20,21] investigated the mechanical behavior of the low-clay translucent whiteware with different slip's solid content. It was found that the maximum flexural strength was ~135 MPa, when the solid content reached

* Corresponding author. Tel.: +86 20 87114217; fax: +86 20 87110273.
E-mail address: sjkescut@163.com (S. Ke).

0272-8842/$36.00
doi:10.1016/j.ceramint.2011.12.028

Table 1
Chemical composition of raw materials.

Raw materials	Constituents (wt.%)								
	SiO_2	Al_2O_3	Fe_2O_3	TiO_2	CaO	MgO	K_2O	Na_2O	Ignition loss
Ball clay	48.61	36.14	0.21	0.14	0.16	0.21	0.98	0.24	12.7
Quartz	98.38	1.02	0.03	0.01	0.08	0.02	0.07	0.04	0.23
Calcite	3.02	0.61	0.04	0.01	53.98	2.13	0.04	0.11	39.82
Alumina	–	≥99.0	–	–	–	–	–	–	–
Feldspar	65.56	18.85	0.08	0.02	0.23	0.03	12.39	2.28	0.56

45 vol.%. However, the cost of preparation was higher than the presently used bone china due to the need for the prefired materials, which were fabricated by highly pure chemical raw materials at 1370 °C. Mineral raw materials have been extensively used for ceramics starting compositions since quite a long time in a large range of possible applications. Taskiran and Capoglu [22,23] reported a new porcelainised stoneware material based on anorthite as porcelainised stoneware tiles, which was obtained from a mixture of wollastonite, alumina, quartz, magnesia and ball clay by powder pressing and sintering at 1225 °C. The material had anorthite as its major phase (~52 wt.%) with corundum (~12 wt.%), cristobalite (~8 wt.%) and glass (~28 wt.%) as minor phases, which had a high degree of whiteness and high-strength (~110 MPa). Nonetheless, corundum was the minor concomitant crystalline phase, which could cause a negative effect on the esthetic properties of anorthite ceramics due to high refractive index (~1.76) [24], compared with anorthite and glassy phases. In the present work, a single crystalline phase ceramic based on anorthite was fabricated from the mineral raw materials such as ball clay, quartz, calcite, feldspar and industrial alumina, without using highly pure chemical raw materials. Properties including phase, microstructures, sintering behavior, flexural strength, thermal expansion and appearance quality were investigated and reported in detail.

2. Experimental procedure

The starting raw materials include ball clay, quartz, and calcite. In order to decrease the firing and crystallization temperature, feldspar was used to obtain dense anorthite-based ceramic at a relatively low temperature. Meanwhile, earlier study [19] demonstrated that the anorthite crystals were only a few microns in length and were not capable enough to resist the pyroplastic deformation during firings. To resist high-temperature deformation, small amount of industrial alumina is added as a source of aluminium to increase the viscosity of melted liquid. All of the starting raw materials were purchased from Guangzhou Sitong Group Co. Ltd. in China. The chemical compositions of the raw materials are shown in Table 1.

The selection of composition is critical to achieve the required crystallization and densification behavior in the final composite. The $CaO–Al_2O_3–SiO_2$ phase diagram shows a broad anorthite forming area in a silica-rich region close to the composition of anorthite [10]. The anorthite region in the phase diagram is surrounded by phases, like mullite ($3Al_2O_3·2SiO_2$), tridymite (SiO_2), wollastonite ($CaO·SiO_2$), gehlenite ($2CaO·Al_2O_3·SiO_2$), $CaO·6Al_2O_3$, and corundum (Al_2O_3). These phases, if formed adversely affect the properties of the final porcelain such as translucency and low thermal expansion coefficient. In this study, the composition of 20 wt.% ball clay, 20 wt.% quartz and 30 wt.% calcite was chosen as the invariable composition while the relative content of feldspar and alumina was changed. A series of compositions were designed in Table 2.

These powders were wet mixed and milled in a planetary mixer with various ratios of zirconia ball millstone for 6 h. The slip casting was used for forming, which could obtain green body with high-strength [25]. The milled slurry was cast in a plaster mold into rectangular blocks of 60 mm × 60 mm × 10 mm dimensions. The consolidated rectangular blocks were removed from the mold after 45 min. Hydration time of the consolidated specimens was determined for 24 h at room temperature in moist atmosphere and then the specimens were dried in an oven for 12 h at 90 °C. Subsequently, the specimens were processed into required shapes and sizes. The different compositions were fired in an electric furnace at 1245 °C firstly. Sintering properties of the fired samples were measured in order to select the optimum formulation. And then the optimum composition was sintered as a function of temperature to identify the best sintering temperature.

The densification parameters in terms of bulk density, water absorption and linear shrinkage were determined by the Archimedes method according to ASTM C373 [26]. The flexural strength of samples were measured by using an electronic universal tester (Model5569, Instron Ltd.) by a three point bending fixture span of 30 mm and cross head speed of 0.5 mm/min. The thermal expansion was measured over the temperature range from 30 to 500 °C using a thermal

Table 2
Composition of the investigated samples (wt.%).

Sample	Raw materials				
	Ball clay	Quartz	Alumina	Feldspar	Calcite
A1	20	20	30	0	30
A2	20	20	27	3	30
A3	20	20	24	6	30
A4	20	20	21	9	30
A5	20	20	18	12	30
A6	20	20	15	15	30
A7	20	20	12	18	30
A8	20	20	9	21	30

dilatometer (NETZSCH DIL 402EP). The property of translucency was measured by ultraviolet–visible spectrophotometer (Unicam, UV-500, USA). The crystalline phases were determined by X-ray diffractometer (Philips PW-1710, Netherlands), using CuKa radiation. The microstructures of samples were observed by scanning electron microscope (SEM, Philips L30FEG, Netherlands).

The whiteness and colors of the final porcelain body were defined using the X-Rite Color Premier 8200 (X-Rite Instruments Ltd., USA), which operates on the CIELab method and in reflection mode. The color coordinates ($L^*a^*b^*$), which specify a color in uniform color space can be measured with this instrument. Each color in the uniform color space can be denoted by three parameters $L^*a^*b^*$ in rectangular coordinates where

L^*: lightness axis, for white $L^* = 100$ and 0 for black;
a^*: red–green axis, positive means red and negative means green;
b^*: yellow–blue axis, positive means yellow and negative means blue.

3. Results and discussions

Fig. 1 shows change in water absorption with different ratios of feldspar and alumina in the fired bodies at 1245 °C for 1 h. The firing temperature is roughly fixed at 1245 °C because the existing composition of transparent glaze can be chosen in this study, which is based on the temperature below 1245 °C. It can be seen from Fig. 1 that the water absorption decreases with increasing ratio of feldspar and alumina and is almost zero in the ratio range 18:12 to 21:9 (samples A7 and A8). The large water absorption with the smaller ratio of feldspar and alumina could be due to undersintering during the firing process at 1245 °C. The small water absorption is attributed to easy

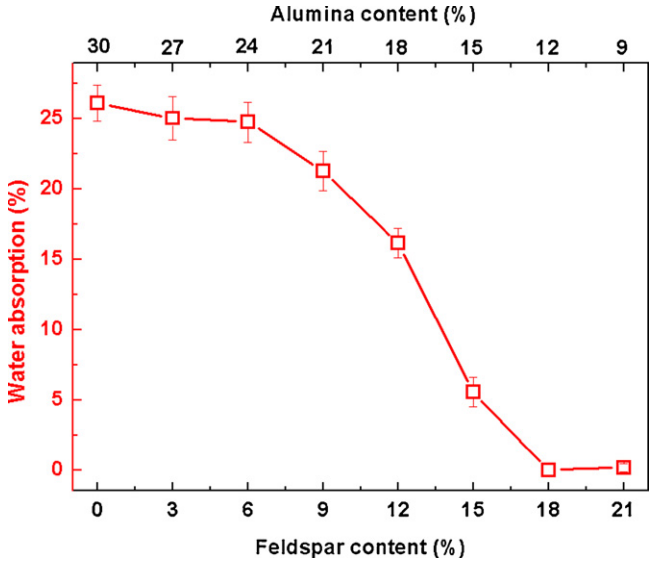

Fig. 1. Change in water absorption with different ratios of feldspar and alumina in the fired samples at 1245 °C.

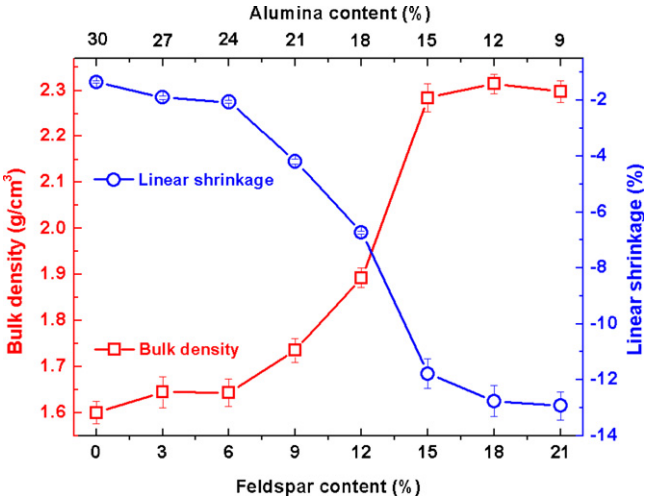

Fig. 2. Change in linear shrinkage and bulk density with different ratios of feldspar and alumina in the fired samples at 1245 °C.

vitrification due to the lowly viscous glass phase during the firing process at all the same temperature. Fig. 2 shows change in linear shrinkage and bulk density with different ratios of feldspar and alumina in the fired bodies at 1245 °C. The linear shrinkage increases with increasing ratio of feldspar and alumina, in conformity with the bulk density. The bulk density exhibits a maximum value with the ratio of feldspar and alumina of 18:12 (sample A7), and the density decreases with higher ratio due to lesser alumina content and the expansion of the closed pores at 1245 °C.

Fig. 3 shows SEM micrographs of polished surface of different samples fired at 1245 °C for 1 h. The samples A3, A4 and A5 contain both isolated large pores and generally interconnected fine pores in large numbers as a result of incomplete densification, which was attribute to higher viscosity of glass phase formed by a large amount of alumina during the firing process [28]. This is demonstrated by comparing the water absorption, consisting with large water absorption at alumina addition of above 15 wt.% as shown in Fig. 1. Moreover, samples A7 and A8 have a relatively small number of large pores due to a large amount of lowly viscous glass phase (Fig. 3e and f).

Fig. 4 shows X-ray diffraction (XRD) patterns of samples A7 and A8 fired at 1245 °C for 1 h. As can be seen from Fig. 4, anorthite is the only crystalline phase in sample A7. Kobayashi and Kato [8] synthesized anorthite from kaolin and $CaCO_3$. Moreover, the crystalline phases of cristobalite, α-quartz and anorthite are observed simultaneously in sample A8. The formation of cristobalite and α-quartz was attributed to the increase of the ratio of SiO_2 and Al_2O_3. In the present study, sample A8, smaller amount of Al_2O_3, possesses higher SiO_2 content in the glass phase dissolved from quartz particles because the highly siliceous glass is formed from larger amount of quartz during the firing process, and the highly siliceous glass is easy to crystallize to cristobalite [25]. Carty and Senapati [29] also argued that cristobalite was formed either from the glass phase or by the direct conversion of quartz. However, a large amount of glassy phase was formed due to

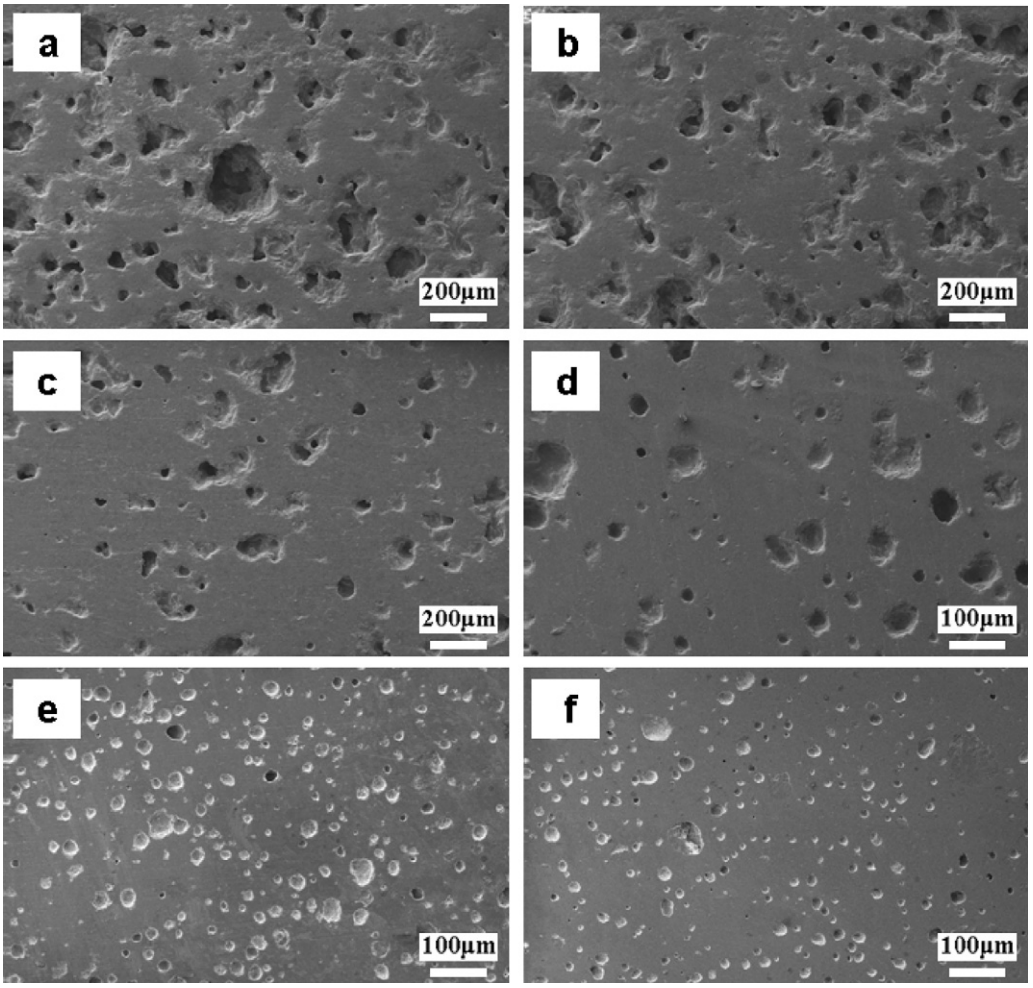

Fig. 3. SEM micrographs of polished surface of different samples fired at 1245 °C. (a) A3, (b) A4, (c) A5, (d) A6, (e) A7 and (f) A8.

higher feldspar content, which could make the strength of this material decrease. On the other hand, according to the presentation mentioned in previous sections, a single crystalline phase ceramic based on anorthite could be good for property of translucency. Hence, the final composition of anorthite-based ceramic was fixed for sample A7.

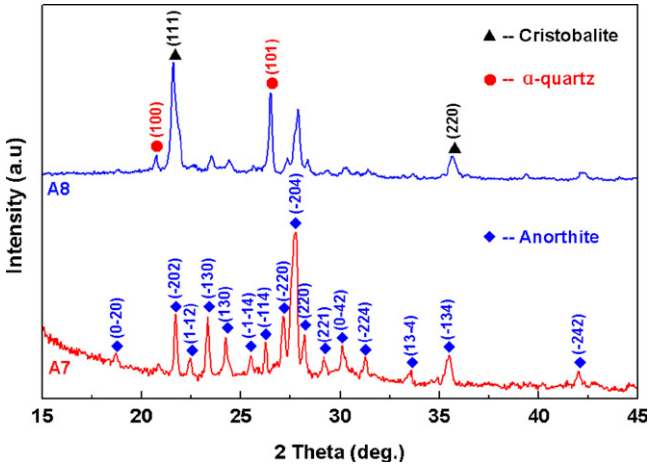

Fig. 4. XRD patterns of samples A7 and A8 fired at 1245 °C.

In order to determine the optimum sintering temperature, densification behavior of sample A7 was studied extensively. Normally, the final fired porcelain would achieve a high degree of densification via partial vitrification at the optimum firing temperature. From the datum given in Table 3, it can be seen that increasing firing temperature had a good effect on the sintering behavior at the temperature below 1230 °C. The ISO 10545 standard prescribes a maximum water absorption value of 0.5 wt.% for porcelain. As shown in Table 3, already at 1230 °C the water absorption became almost zero indicating that the fired body achieves of the standard's requirement. Sample A7 sintered at 1230 °C shows a maximum density of 2.41 g/cm^3, which is about 87% of theoretical density (2.76 g/cm^3) [34]. Further heating the density decreased, but the water absorption value reached zero. In essence, density is brought about primarily by the structure in porosity for the same composition material. Fig. 5 shows SEM micrographs of polished surface of sample A7 fired at different temperatures. Clearly, the average pore size decreased with an increase in sintering temperature up to 1230 °C, where it attained its minimum. Later, the pore size had a trend of turning large at 1245 °C, which was attributed to expansion of the entrapped gases such as CO_2, CO and N_2 [27], leading to the decrease in

Table 3
Sintering character and flexural strength of sample A7 fired at different temperatures.

Property	Temperature (°C)			
	1170	1200	1230	1245
Water absorption (%)	13.98 ± 3.03	5.82 ± 1.63	0.25 ± 0.01	0.00 ± 0.00
Apparent porosity (%)	30.14 ±3.36	13.19 ± 0.73	1.16 ± 0.01	0.00 ± 0.00
Bulk density (g/cm^3)	1.89 ± 0.02	2.27 ± 0.03	2.41 ± 0.02	2.31 ± 0.02
Relative density (%)	68.5	82.2	87.3	83.7
Flexural strength (MPa)	49.8 ± 3.7	74.3 ± 3.3	103.7 ± 4.1	93.6 ± 5.3

density. Furthermore, water absorption is closely related to apparent porosity in theory. The water absorption and apparent porosity show a similar changing trend in Table 3. Thus, the open pore of sample A7 became smaller while closed pore increased gradually in the temperature range from 1230 to 1245 °C.

Table 3 also shows the flexural strength behavior of sample A7 as a function of sintering temperature. It can be seen that a sharp increase in strength was observed at sintering temperatures of 1170–1230 °C, and the strength values decreased as the temperature was increased above this range, similarly affecting like literature [27]. Flexural strength showed a consistent relation with bulk density, as expected. A maximum flexural strength of 103 MPa was observed at 1230 °C, which is higher than that of the conventional porcelain. Besides, the phase compositions have a significant effect on the flexural strength behavior of porcelain [17–23]. The XRD patterns in Fig. 6 reflect the crystallization trend of sample A7 fired at different temperatures for 1 h. It can be seen that anorthite is always the major phase in the temperature range from 1170 to 1245 °C. When the sample A7 was fired at the temperature below 1230 °C, a small amount of corundum crystalline phase was shown in Fig. 6a and b. And the peak of corundum decreased with increasing temperature and disappeared above 1230 °C. The peak intensities of anorthite phase increased up to a maximum at 1230 °C, at this temperature only a single anorthite phase was obtained (Fig. 6c). In another work [9], it has reported that single phase anorthite ceramic could be obtained from sintering of raw materials with coarse particles at 950 °C by using boron oxide addition. In this study, feldspar addition leads to formation of single anorthite phases at lower temperature. In addition, the curves b and d appeared a broad peak, respectively, which associated with amorphous phase. It means that there exists quite an amount of glass phase, compared with crystalline phase quantity. The previous literature [30–33] also implied that anorthite could be formed

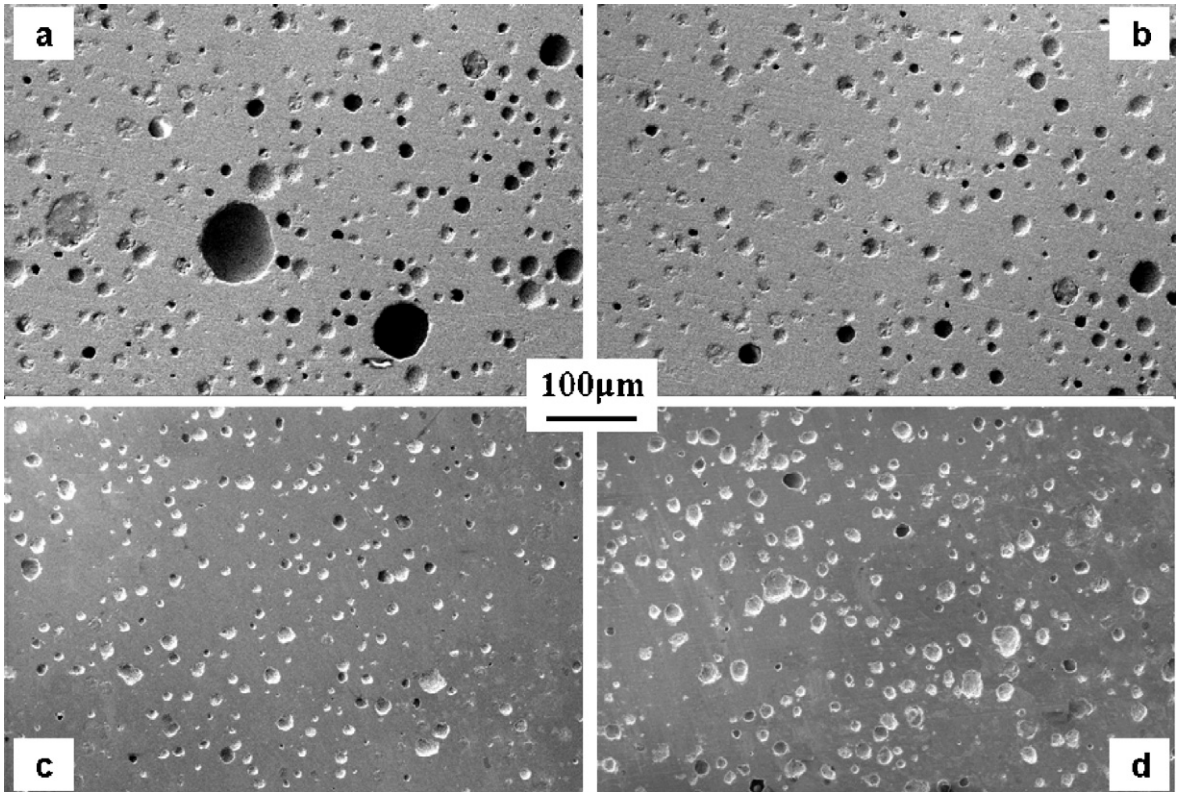

Fig. 5. Pore structures of sample A7 fired at (a) 1170 °C, (b) 1200 °C, (c) 1230 °C and (d) 1245 °C.

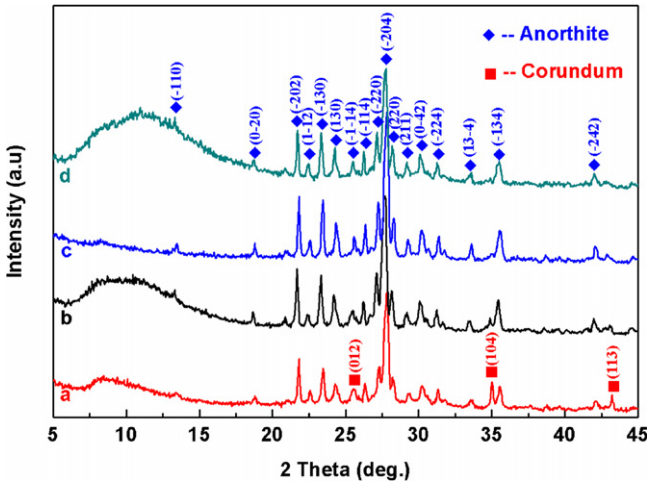

Fig. 6. XRD patterns of sample A7 fired at (a) 1170 °C, (b) 1200 °C, (c) 1230 °C, and (d) 1245 °C.

by the crystallization from the glassy phase during the firing process. On the other hand, the viscosity of glassy phase is quite rapidly decreased at about 1245 °C and the decreased viscosity of liquid phase makes anorthite particles melt easily leading to the increase of glassy phase. Above knowable, sample A7 has single crystalline phase and the optimum sintering performance at the temperature of 1230 °C.

Fig. 7 is the SEM micrographs of fracture surface of sample A7 fired at 1170 °C, 1200 °C, 1230 °C, 1245 °C for 1 h, respectively. Clearly, characteristic cuboid or lamellar crystals of anorthite were seen and the average grain sizes increased with increasing firing temperature. Marques and Tulyaganov [35] also fabricated the anorthite crystals with similar shape from a CaF_2–CaO–Al_2O_3–SiO_2–MgO–P_2O_5–B_2O_3 system process in the temperature range of 850 to 950 °C. Comparing Fig. 7b–d, the preparation of the samples for SEM observation by chemical etching with HF solution allowed us to draw out qualitative conclusions about the content of the residual glass phase, and it was found that it follows the general order $c < b$, $c < d$. So, the sample A7 fired 1230 °C possessed a high crystalline to glass ratio. The high flexural strength of anorthite-based ceramic also might be due to the formation of high crystalline content in the matrix of the ceramic body, which is consistent with the previous research results [20–23].

The thermal expansion coefficient is a key factor when considering the thermal matching between glaze and body [36]. The thermal expansion behavior of simple A7 fired at 1230 °C for 1 h was measured between room temperature and 500 °C as shown in Fig. 8. The expansion ratio is almost linear increase over the entire measured temperature range. The ceramic body exhibits only slow expansion when it is heated, which means that all the thermal expansion coefficients (TEC) are positive. For practical application of high-strength porcelain for table-

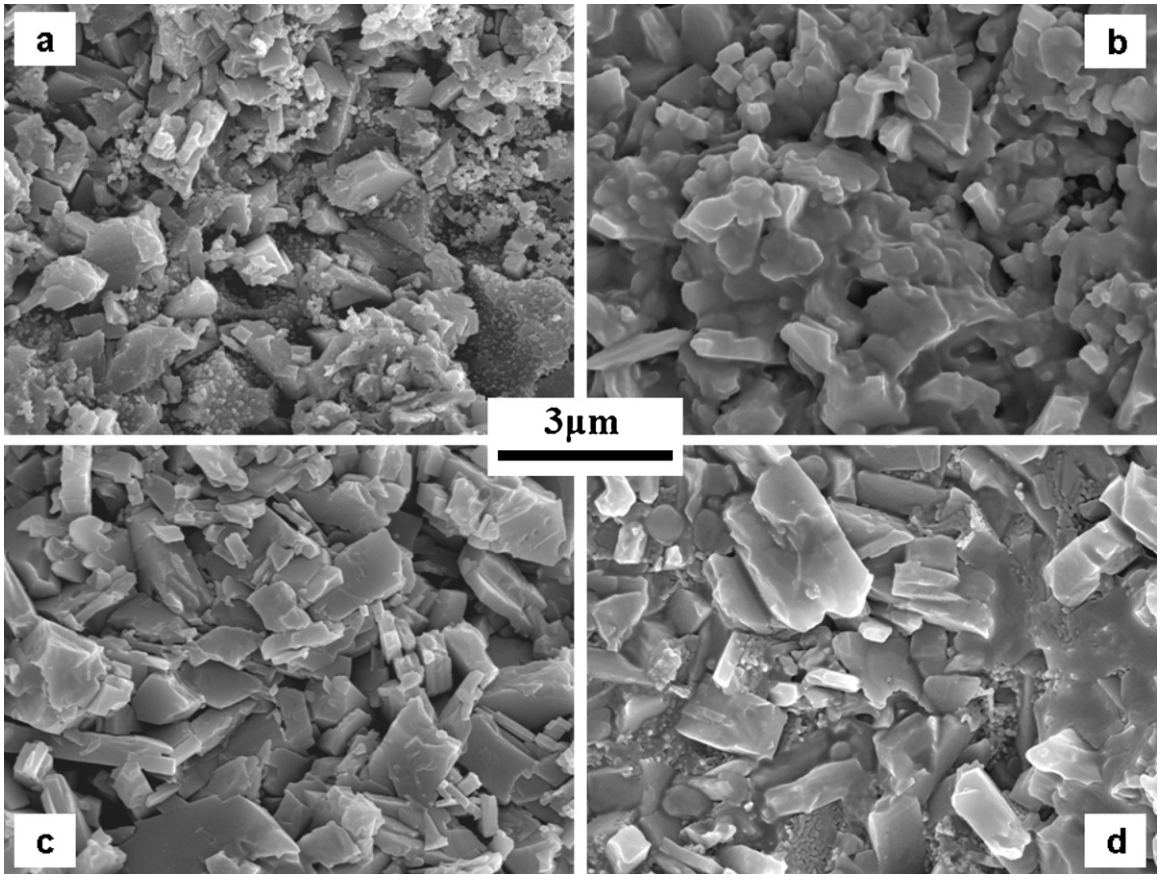

Fig. 7. SEM micrographs of fracture surface of sample A7 fired at (a) 1170 °C, (b) 1200 °C, (c) 1230 °C, and (d) 1245 °C.

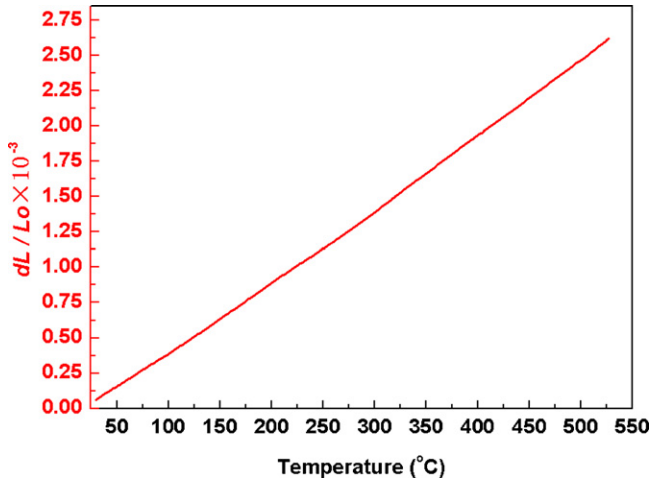

Fig. 8. Thermal-expansion ratio curve of anorthite-based ceramic as a function of temperature.

Table 4
Average TEC of the anorthite-based ceramic in various ranges of temperature.

Temperature (°C)	TEC ($\times 10^{-6}$ K^{-1})
30–100	4.6472
30–200	4.8745
30–300	4.9142
30–400	5.0601
30–500	5.1189

ware, thermal expansion below 150 °C is important in order to withstand the thermal shock of heat disinfection or washing [37]. According to thermal expansion coefficients, the average TEC values of all the simples in the area of the tested temperature are calculated and listed in Table 4. From the table, the TEC of anorthite-based ceramic below 300 °C were calculated as 4.91×10^{-6} K^{-1}, which is similar with the porcelainised stoneware material based on anorthite [22]. According to simple rule of mixture [38], the value of TEC could be calculated by using simple rule of mixtures which is consistent with the relative proportions of the phases. Anorthite-based ceramic has a low TEC value due to formation of a single anorthite phase, whose TEC value is $\sim 4.3 \times 10^{-6}$K^{-1} from 20 to 500 °C [39]. While the TEC for glasses of the compositions detected in common glaze from 20 to 350 °C were calculated to be 3–4.5 $\times 10^{-6}$ K^{-1} [38]. So, the anorthite-based ceramic can be matched with applicable glaze easily. Moreover, this relatively low TEC also indicates that the materials would be very resistant to being thermally shocked.

Table 5
Degree of whiteness of anorthite-based ceramic, bone china and anorthite-based porcelainised stoneware.

Type of porcelain	Source	L^*	a^*	b^*
Bone china	[19]	93.15	−0.43	3.17
Anorthite-based porcelainised stoneware	[22]	91.05	−1.31	4.85
Anorthite-based ceramic	This work	94.37	−0.54	1.92

The appearance quality of tableware is crucial for its marketing. As a ceramic material bone china is a highly specialized product and is the basis of the world's most attractive and expensive types of tableware, mainly due to excellent appearance quality such as translucency and whiteness [40]. In the present study, the color was measured by using a spectrometer used in the reflection mode. It operates on the CIELab color space system in which the color descriptors are L^*, a^*, and b^*. The $L^*a^*b^*$ system was chosen for this study because it best quantifies color as perceived by the human eye [41].

In modern technology for the production of vitrified porcelain ware, particularly for tableware, greater attention is paid to the industrial development of white base body [42]. In order to explain quantitatively the degree of whiteness of the anorthite-based ceramic, the differences of the anorthite-based ceramic and the other two types of whiteware, namely bone china [19] and anorthite-based porcelainised stoneware [22], were compared. The color difference values (a^*, b^*) and the L^* parameters (whiteness) are summarized in Table 5. It can be seen from Table 5 that negative value of a^* and positive value of b^* were measured from anorthite-based ceramic, indicating that the values lie in the upper left quadrant (green and yellow region) with coordinates. It also appears evident that the value of b^* is the smallest of the three types of porcelain and the value of a^* is similar with bone china, which indicates that the new anorthite-based ceramic has very shallow mottles. Meanwhile, the degree of whiteness of the anorthite-based ceramic can be reached ~94, which is higher than that of bone china (~93) and anorthite-based porcelainised stoneware (~91). The new anorthite-based ceramic owes its high degree of whiteness to the usage of raw materials containing low coloring impurities such as Fe_2O_3 and TiO_2. So the porcelain based on anorthite has a high appearance quality similar to that of bone china.

The translucency behavior of anorthite-based ceramic is shown in Fig. 9. There is a photograph of the surface-polished simple with 2 mm thickness in the top right corner of Fig. 9,

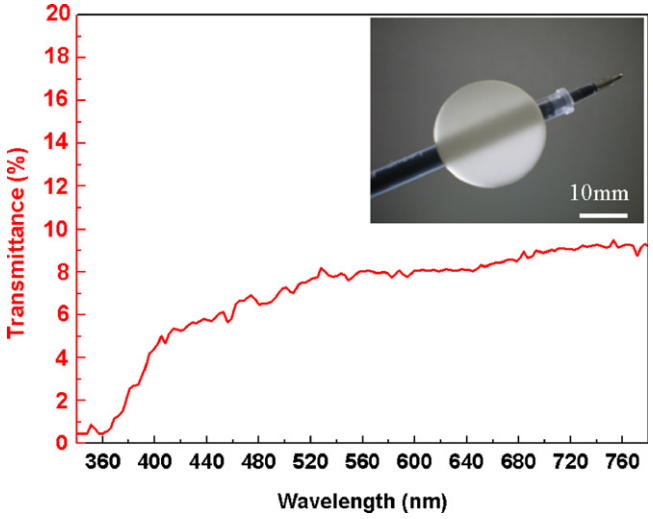

Fig. 9. Translucency sample and transmittance curve of polished anorthite-based ceramic slice in the visible spectral range.

which appears a good translucency appearance since the ballpoint pen can be seen through the ceramic body. Theoretically, the translucency behavior of material is related to light scattering, which can cause a bad influence on transmittance. In general, light scattering can occur at grain boundaries where refractive indices are discontinuous. This is especially easy for noncubic structures. A similar situation can occur in multiphase materials, such as ceramics densified by liquid-phase sintering, where there may be an intergranular film. For the traditional ceramic, matching refractive indices between different phases can reduce scattering losses. This approach is used in making high-quality bone china [24]. In order to illustrate quantitatively translucency of anorthite-based ceramic, visible light transmittance of polished sample with 1 mm thickness was measured by ultraviolet–visible spectrophotometer. The result shows that the optical transmittance of anorthite-based ceramic increased with increasing wavelength and the average transmittance is about 7% in the visible spectral range, which has a similar decoration quality to that of bone china due to the low relative refractive index between anorthite (∼1.58) [15] and glassy phase (∼1.51) [16]. In addition, other studies [22,23] reported a new porcelainised stoneware material based on anorthite, whose phases were anorthite, corundum, cristobalite and glass. However, multiphase could cause a negative effect on the translucency behavior because of the difference in refractive index of multiphase.

Furthermore, the cost of anorthite-based ceramic could be lower than the presently used bone china due to using the common mineral raw materials. And it has the same simple process as the present industry. It is believed that the new material will have a significant contribution to daily porcelain industry.

4. Conclusions

In this study, anorthite-based ceramic was fabricated by slip casting and sintering from the mineral raw materials. Microstructures and properties including flexural strength, thermal expansion and appearance quality were discussed. It was found that the single phase anorthite ceramic was obtained at 1230 °C for 1 h. Sintering temperature played a major role in the change of the phases and microstructures, and the optimized sintering temperature of 1230 °C was found to best sintering properties. The single phase anorthite ceramic has a high flexural strength of 103 MPa, which is higher than that of the conventional porcelain. It was attributed to obtaining a density of 87% of the theoretical density and high crystalline to glass ratio. The single phase anorthite ceramic had relatively low ($4.9 \times 10^{-6}\ K^{-1}$) thermal expansion coefficient which can be matched with applicable glaze easily. Moreover, this relatively low TEC also can be very resistant to being thermally shocked.

The single phase anorthite ceramic had high degree of whiteness ($L^* = 94$) and excellent translucency behavior which could achieve a high-quality decorative effect due to the low relative refractive index between anorthite and glassy phase. Furthermore, the properties of the single phase anorthite ceramic are extremely excellent and it has the same simple process as the present industry. It is believed that the new material will have a significant contribution to daily porcelain industry.

Acknowledgement

This work was supported by the Major Scientific and Technological Projects of Guangdong Province (No. 2010A080804001) and the ChanXueYan Special Funds of Guangdong (No. 2011B090400201).

References

[1] S. Mucahit, A. Sedat, Utilization of recycled paper processing residues and clay of different sources for the production of porous anorthite ceramics, J. Eur. Ceram. Soc. 30 (2010) 1785–1793.
[2] R.A. Gdula, Anorthite ceramic dielectrics, Am. Ceram. Soc. Bull. 50 (1971) 555–557.
[3] M.R. Boudchicha, S. Achour, A. Harabi, Crystallization and sintering of cordierite and anorthite based binary ceramics, J. Mater. Sci. Lett. 20 (2001) 215–217.
[4] B. Ryu, I. Yasui, Sintering and crystallization behavior of a glass powder and block with composition of anorthite and microstructure dependence of its thermal expansion, J. Mater. Sci. 29 (1994) 3323–3328.
[5] S. Kavalci, E. Yalamac, S. Akkurt, Effects of boron addition and intensive grinding on synthesis of anorthite ceramics, Ceram. Int. 34 (2008) 1629–1635.
[6] S. Agathopoulos, D.U. Tulyaganov, P.A. Marques, M.C. Ferro, M.H. Fernandes, R.N. Correia, The fluorapatite anorthite system in biomedicine, Biomaterials 24 (2003) 1317–1331.
[7] S. Lee, G. Kim, Characteristics and densification behavior of anorthite powder synthesized by a solution process employing a polymer carrier, J. Ceram. Process. Res. 3 (2002) 136–140.
[8] Y. Kobayashi, E. Kato, Low-temperature fabrication of anorthite ceramics, J. Am. Ceram. Soc. 77 (1994) 833–834.
[9] A. Mergen, Z. Aslanoglu, Low-temperature fabrication of anorthite ceramics from kaolinite and calcium carbonate with boron oxide addition, Ceram. Int. 29 (2003) 667–670.
[10] E.M. Levin, C.R. Robbins, H.F. Mcmurdie, Phase Diagrams for Ceramists, The American Ceramic Society, Columbus, OH, 1975.
[11] B. Bulent, S. Yuksel, A. Tulay, O. Muserref, The effect of boron containing frits on the anorthite formation temperature in kaolin–wollastonite mixtures, J. Eur. Ceram. Soc. 23 (2003) 2061–2066.
[12] A. Guechi, S. Achour, A. Harbi, Effect of temperature and Na_2CO_3 addition on sintering and crystallisation of anorthite, Key Eng. Mater. 264-268 (2004) 257–260.
[13] A. Mergen, T.S. Kayed, M. Bilen, A.F. Oasrawi, M. Guru, Production of anorthite from kaolinite and $CaCO_3$ via colemanite, Key Eng. Mater. 264-268 (2004) 1475–1478.
[14] K. Sedat, Y. Emre, A. Sedat, Effects of boron addition and intensive grinding on synthesis of anorthite ceramics, Ceram. Int. 34 (2008) 1629–1635.
[15] D.R. Lide, CRC Handbook of Chemistry and Physics, 72nd ed., CRC Press, Boston, 1992.
[16] C.E. Meloan, R.E. James, R. Saferstein, Refractive Index of Glass Fragments, Criminalistics: An Introduction to Forensic Science, Lab Manual, 6th ed., Upper Saddle River, NJ, Prentice-Hall, 1998, pp. 29–35.
[17] A. Capoglu, P.F. Messer, Design and development of a chamotte for use in a low-clay translucent whiteware, J. Eur. Ceram. Soc. 24 (2004) 2067–2072.
[18] A. Capoglu, A novel approach to high-strength, translucent whiteweras using prefired materials, Key Eng. Mater. 264-268 (2004) 1585–1588.
[19] A. Capoglu, A novel low-clay translucent whiteware based on anorthite, J. Eur. Ceram. Soc. 31 (2010) 321–329.

[20] A. Capoglu, M.U. Taskiran, Fabrication of low-clay containing translucent whiteweras using prefired materials by slips casting, Key Eng. Mater. 264-268 (2004) 1621–1624.
[21] C.B. Ustundag, Y.K. Tur, A. Capoglu, Mechanical behavior of a low-clay translucent whiteware, J. Am. Ceram. Soc. 26 (2006) 167–177.
[22] M.U. Taskiran, N. Demirkol, A. Capoglu, A new porcelainised stoneware material based on anorthite, J. Eur. Ceram. Soc. 25 (2005) 293–300.
[23] A. Capoglu, M.U. Taskiran, Processing of ultra white porcelain stoneware based on anorthite, Key Eng. Mater. 264–268 (2004) 1495–1498.
[24] C.B. Carter, M.G. Norton, Interacting with and generating light, Ceram. Mater. Sci. Eng. VII (2007) 575–597.
[25] P.T. Weon, K. Kimura, K. Jinnal, Fabrication of new porcelain body using nonplastic raw materials by slip casting, J. Mater. Sci. 37 (2002) 1273–1279.
[26] Annual Book of ASTM Standards, 2000, C-20, Standard Test Methods for Apparent Porosity, Water Absorption, Apparent Specific Gravity and Bulk Density of Burned Refractory Brick Shapes by Boiling Water.
[27] S. Maity, B.K. Sarka, Development of high-strength whiteware bodies, J. Eur. Ceram. Soc. 16 (1996) 1083–1088.
[28] Y. Iqbal, W.E. Lee, Microstructural evolution in triaxial porcelain, J. Am. Ceram. Soc. 83 (2000) 3121–3127.
[29] W.M. Carty, U. Senapati, Porcelain-raw materials, processing, phase evolution, and mechanical behavior, J. Am. Ceram. Soc. 81 (1998) 3–20.
[30] K. Andreas, H. Thomas, K. Jens, Transmission physics and consequences for materials selection, manufacturing, and applications, J. Eur. Ceram. Soc. 29 (2009) 207–221.
[31] P. Rado, Bone China, Ceramic Monographs, Handbook of Ceramics, Verlag Schmid GmbH, Freiburg i. Brg., 1981.
[32] R.K. Wood, Ceramic whiteware, ceramics and glasses, engineered materials handbook, ASM International, 1991, pp. 930–936.
[33] S.A.F. Batista, P.F. Messer, R.J. Hand, Fracture toughness of bone china and hard porcelain, Br. Ceram. Trans. 100 (2001) 256–259.
[34] S. Kurama, E. Ozel, The influence of different CaO source in the production of anorthite ceramics, Ceram. Int. 35 (2009) 827–830.
[35] V.M.F. Marques, D.U. Tulyaganov, S. Agathopoulos, V.Kh. Gataullin, G.P. Kothiyal, J.M.F. Ferreira, Low temperature synthesis of anorthite based glass-ceramics via sintering and crystallization of glass-powder compacts, J.Eur. Ceram. Soc. 26 (2006) 2503–2510.
[36] H.L. Tang, J. Xua, H.J. Lia, Y.J. Dong, F. Wu, M.Q. Chen, Structure, thermal expansion and optical property of alumina-rich spinel substrate, J. Alloys Compd. 479 (2009) 26–29.
[37] K. Yuichi, Y. Mitsunori, N. Mikio, O. Osamu, I. Hirofumi, Strength and thermal shock resistance of alumina-strengthened porcelain containing cristobalite, J. Ceram. Soc. Jpn. 111 (2003) 872–877.
[38] A. Capoglu, Elimination of discoloration in reformulated bone china bodies, J. Eur. Ceram. Soc. 25 (2005) 3157–3162.
[39] L. Barbieri, F. Bondioli, I. Lancellotti, C. Leonelli, M. Montorsi, The anorthite–diopside system: structural and devitrification study. Part II. Crystallinity analysis by the rietveld-RIR method, J. Am. Ceram. Soc. 88 (2005) 3131–3136.
[40] A. Kara, R. Stevens, Characterisation of biscuit fired bone china body microstructure. Part I. XRD and SEM of crystalline phases, J. Am. Ceram. Soc. 22 (2002) 731–736.
[41] S.A. Berger, Practical Color Measurement: A Primer for the Beginner, A Reminder for the Expert, John Wiley, New York, 1994.
[42] Kr.D. Swapan, D. Kausik, Differences in densification behavior of K- and Na–feldspar-containing porcelain bodies, Thermochim. Acta 406 (2003) 199–206.